THE GENETIC BASIS FOR THE FIRST CONNECTIONS IN THE BRAIN

by

ANISHA ADKE

A THESIS

Presented to the Department of Biology
and the Robert D. Clark Honors College
in partial fulfillment of the requirements for the degree of
Bachelor of Science

June 2018

An Abstract of the Thesis of

Anisha Adke for the degree of Bachelor of Science
in the Department of Biology to be taken June 2018

Title: The genetic basis for the first connections in the brain

Approved: _____

Adam C. Miller

An estimated 100 billion neurons form the human brain, equal to the number of stars in the Milky Way Galaxy. Nervous system function emerges from the patterns and properties of the connections, or synapses, between these neurons. Synapses come in two broad types, electrical, with direct communication mediated by gap junctions, or chemical, with indirect communication facilitated by neurotransmitter release and reception. These synapses form a neural circuit that emerges over development, initially directed by an organism's genetic code. The first synapses that form are critical to normal circuit wiring, as they lay the foundation upon which mature circuits are built. While we know that these first synapses are electrical, it is unknown which genes are responsible for creating these first connections. This project aimed to identify the connexins responsible for the first synapses and investigate their roles from a neural circuit and behavioral standpoint. This will provide a critical understanding of nervous system wiring, as genetic defects that alter normal circuit wiring are linked to neurodevelopmental disorders such as autism and schizophrenia.

To explore the genes responsible for electrical synapses, we examined the first spinal cord circuits that form in zebrafish. Because nearly 85% of disease-

associated genes are conserved between zebrafish and humans, zebrafish are an ideal model system. Additionally, neurons and synapses of the spinal circuits are easily accessible to investigation throughout development. Day-old zebrafish exhibit spontaneous coiling, a behavior that requires electrical synapses between neurons of the spinal cord. We hypothesized that disrupting genes involved in electrical synapse formation would disrupt coiling behavior, providing a convenient proxy for finding the genes involved in circuit formation. We mutated electrical synapse genes and analyzed coiling behavior to find how, when, and where these genes control the formation of the first synapses. Behavioral analysis suggests that the gene *gjd4*/Cx46.8 is involved in early circuit formation while mutations in *gjd2b*/Cx35.1*, gjd1a*/Cx34.1*, gjd2a*/Cx35.5*, gjd1b*/Cx34.7*,* and *gjc2*/Cx43.4 had no effect on coiling behavior. Future directions will center around where *gjd4*/Cx46.8 is expressed in the spinal cord and to understand how it influences neural circuit formation and function by using fluorescent calcium indicators.

Acknowledgements

I would like to thank Professor Adam Miller for mentoring me for the past three years in his lab. He has spent countless hours teaching me techniques, meeting with me to talk through this project, supporting me, and encouraging me to grow as a scientist. I feel grateful to have had his mentorship and friendship for the past few years.

The other members of the Miller lab, particularly Jen Michel and Audrey Marsh for answering all of my questions and for training me when I first joined the lab. I have appreciated their expertise and willingness to help me learn.

I would also like to acknowledge the UO Fish Facility Staff, especially Tim Mason and Marcy McFadden. I thank them for making sure our zebrafish were always well taken care of and for accommodating the early morning behavioral experiments that this project required.

I would also like to thank Professors Rebecca Lindner and Terry Takahashi for serving on my thesis committee and for both teaching some of my favorite classes that I took during my college career. I appreciate both of their support during this process.

Finally, I would like to recognize the Clark Honors College and the Biology Department for providing me with the opportunity to write a thesis on my work. In particular, I'd like to thank Dr. Kryn Stankunas for the guidance all year and Miriam Jordan for her work in coordinating theses in the Honors College.

Table of Contents

List of Figures

List of Tables

Introduction

The nervous system is composed of discrete, communicating cells

In 1852, Santiago Ramón y Cajal was born to a father who strongly discouraged pursuing the arts. Instead, and fortunately for the neuroscience community, his father pushed him to attend medical school. At the time that Ramón y Cajal was educated and began working, the widely accepted view of the nervous system was that it consisted of a single large, continuous nerve net. This viewpoint, known as Reticular Theory, was supported by Camillo Golgi, a scientist who had developed a method of staining and visualizing neurons using silver. His results highlighted individual neuronal projections, but could not definitively determine whether neurons were uninterrupted networks or separate cells. Ramón y Cajal, upon learning of Golgi's staining method, modified the technique to improve resolution and inferred that the nervous system was made up of many neurons separated by microscopic gaps. Using this finding, Ramón y Cajal coined the Neuron Doctrine, which opposed Golgi's Reticular Theory of nerve nets. Instead, Ramón y Cajal postulated that the nervous system was composed of discrete cells that propagate signals throughout the body by transferring information from neuron to neuron. Through his meticulous drawings of both individual neurons as well as complex circuits, Ramón y Cajal's findings suggested for the first time the existence of intricate neural circuits that compose the nervous system and give rise to function (Figure 1). In 1906, Golgi and Ramón y Cajal were jointly awarded the Nobel Prize in Physiology and Medicine to recognize both of their vital contributions to understanding the nervous system (De Carlos and Borrell, 2007, Golgi and Ramón y Cajal, 1906). Since Ramón y

Cajal and Golgi's time, scientists have categorized neurons into at least a thousand different types that can be classified into 3 broad categories: 1) sensory neurons convert external stimuli into internal signals, allowing an organism to receive information from the outside world, 2) interneurons transmit information between neurons allowing for neuronal communication, and 3) motorneurons pass information from neurons to muscle cells to invoke contraction or relaxation, translating the internal processes of the brain into external action. These three essential types of neurons wire together into enormous arrays of circuits that underlie behavior (Kandel et al., 2014).

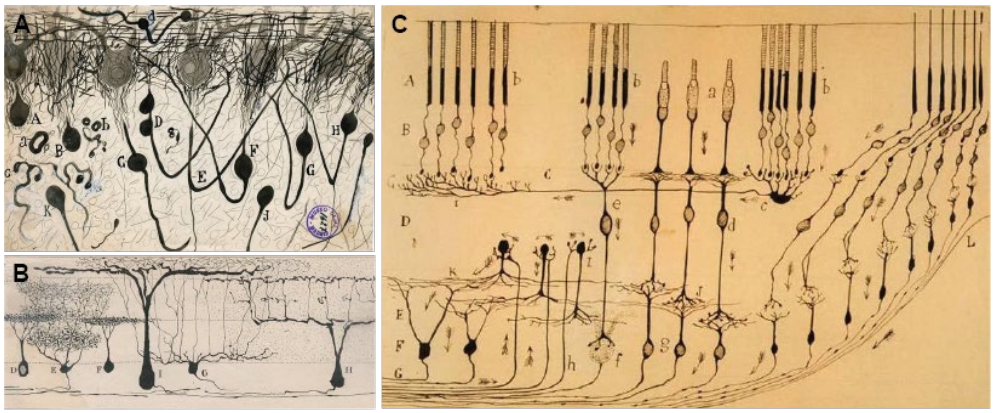

Figure 1. Neural diversity and connectivity, drawn by neuroscientist Santiago Ramón y Cajal.

A) Axons of Purkinje neurons and basket fibers in the adult, human, male cerebellum. B) Retinal neurons in the lizard. C) Retinal neurons in humans. Each layer, made up by discrete cells, make connections with one another to transmit information. For example, rod photoreceptors (cell type b, sensory neurons) connects with horizontal cells (type c, interneuron), which connect different rod cells across space to give rise to lateral inhibition, a mechanism that fine-tunes humans' ability to perceive a light source. Bipolar cells (type E) carry information between photosensitive rod cells and the retinal ganglion cells (type F, interneuron) that then carry information into the brain. This connectivity between retinal neurons gives rise to complex functions and behaviors inherent to vision. All drawings from the Cajal Institute, Madrid.

Neural circuits are the basis of behavior

Although Ramón y Cajal found that neurons were separate entities, it took another half century to characterize the connective structures that formed the conduits of neuronal communication. These structures, now called **synapses** connect neurons together and give rise to neural circuits that allow for all behaviors, from simple escape responses to complex emotions. For example, fast escape responses in zebrafish are facilitated by Mauthner interneurons, which receive electrical stimuli from sensory neurons and send information to motorneurons, thus forming a neural circuit. When a threatening stimulus is detected, the zebrafish can rapidly activate a motor response and

quickly turn and swim away (Tabor et al., 2014). In this case, touch-, sound-, and light-sensitive sensory neurons in the peripheral sensory organs connect with the Mauthner interneuron, whose axon stretches down the length of the spinal cord. When external stimuli activate sensory neurons, the signal travels down the sensory neurons and activates the Mauthner interneuron communicating via synapses. Mauthner then relays the message through the hindbrain and down the spinal cord where it connects with motorneurons. Activation of the motorneurons causes muscular contractions on one side of the zebrafish's body, pivoting the fish away from the stimulus and danger. The circuit formed by these three neuron types allow for the escape response. This simple model circuit provides a glimpse into how neurons can be organized to produce a function. Although this circuit is simple, the same notion is mirrored in how billions of connections in the human cortex form the basis for complex thought, behaviors, and emotions.

Neurons and synapses are the building blocks of the brain

Since Ramón y Cajal's time, scientists have found that neurons are specialized cells that communicate by receiving and transmitting electrical signals, analogous to how a computer functions through wired circuits. Instead of electrons flowing through the wires of a computer, neurons use ions and other small molecules to communicate. In 1952, Alan Hodgkin and Andrew Huxley wrote a series of five articles describing how an electrical impulse traveled along the length of a neuron and defined mathematical models for ion movement in neurons during communication. Their experiments on the squid giant axons showed how **voltage-gated ion channels** produce propagating signals (Hodgkin & Huxley, 1952).

An action potential, or an increase in voltage inside the neuron that serves as the electrical communication signal, is received in the **dendrites** of a **presynaptic** neuron (Figure 2). The voltage change is propagated from the receiving dendrites into the cell body, which it travels through and triggers ion channels along the neuron's **axon** to open and allows sodium to enter the cell, which continues the depolarization along the length of the neuron (Kandel et al., 2014 and Hodgkin & Huxley, 1952). Once the action potential reaches the **axon terminal**, the impulse encounters a synapse. In chemical synapses, the local depolarization triggers voltage-gated calcium channels to open. Calcium then flows into the cell and binds to proteins that initiate a signal cascade to facilitate **neurotransmitter** release. Synaptic vesicles, or packets of neurotransmitter, are pulled close to the membrane of the axon terminal by proteins that membrane fusion. When the outer casing of the vesicle fuse with the lipid membrane of the neuron in a process called exocytosis, neurotransmitter is deposited into the synaptic cleft to diffuse and bind with receptors on the **postsynaptic cell**. When the neurotransmitter is received, it prompts voltage changes in the receiving neuron that causes channels to open on the postsynaptic cell, sodium to flow in, and the process to repeat (Kandel et al., 2014).

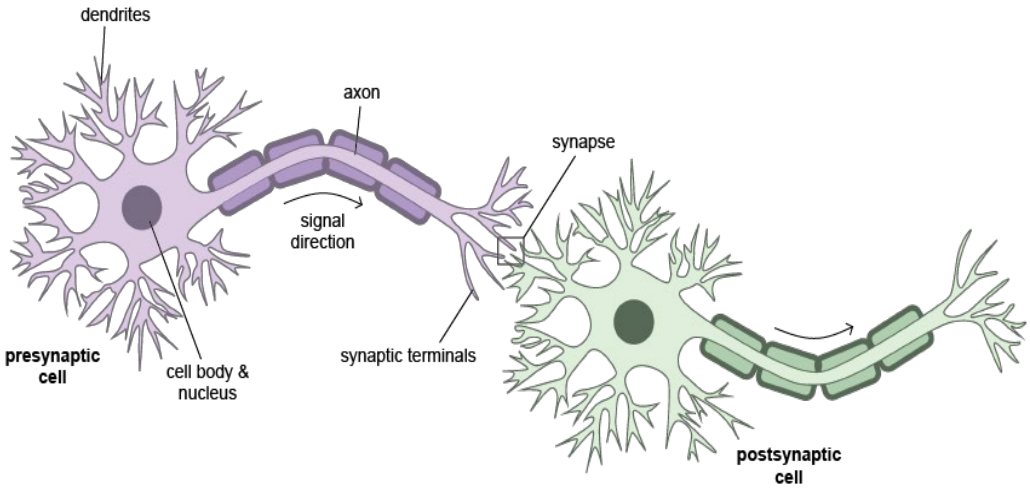

Figure 2. The structure of a neuron.

Electrical signals (action potentials) enter a cell through its dendrites. The signal then passes through the cell body and travels down the axon to the synaptic terminal, where it passes the impulse to a postsynaptic cell. Note that the dendrites of the presynaptic cell connects with other neurons (not shown for clarity).

While chemical synapses account for a large amount of neuronal communication in the human brain, electrical synapses are also an essential method used in neuronal communication. Electrical synapses have a particularly vital role during brain development (Peinado et al., 1993; Nadarajah et al., 1997; Chang and Balice-Gordon, 2000; Roerig and Feller, 2000). When the depolarization reaches the synaptic terminal, rather than neurotransmitter being released into the synaptic cleft, at electrical synapses the two neighboring neurons are directly linked through **gap junction channels** (Figure 3A, B). Gap junction channels are formed by two hemi-channels, one associated with either the presynaptic or the postsynaptic cell. Each hemi-channel is composed of six protein subunits, or called **Connexins**. The gap junction channels cross the membranes of both cells to form a pore wide enough to allow ions and small signaling molecules to pass directly from one cell to the next. Because they are directly coupled, when one

cell's membrane potential changes, ions flow through one cell to the next, carrying that change in potential with them to the postsynaptic cell (Kandel et al., 2014).

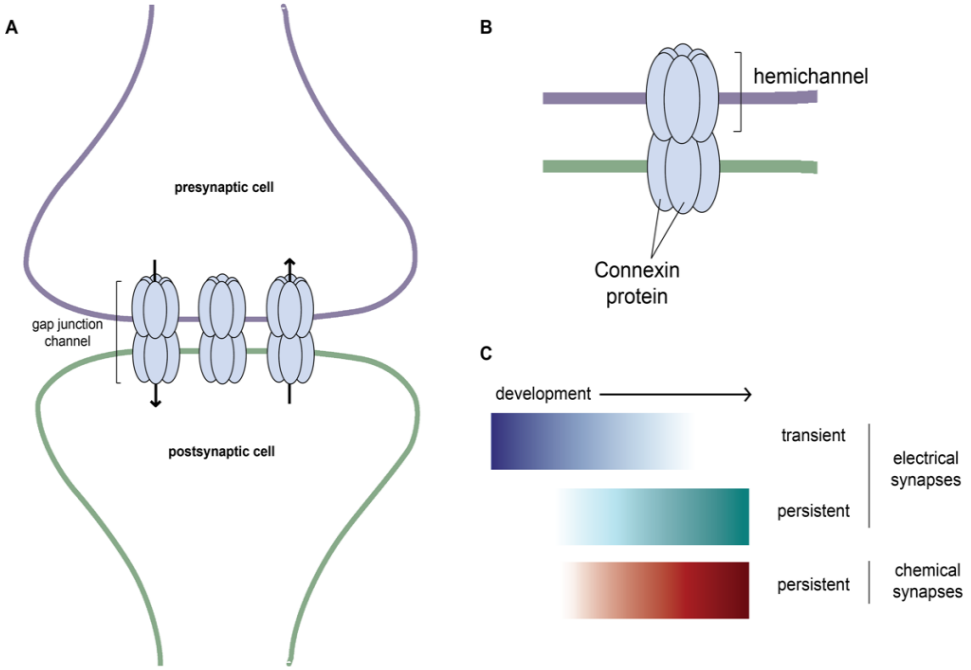

Figure 3. The structure of electrical synapses.

A) Electrical synapses directly couple a presynaptic and postsynaptic neuron through gap junction channels. The diffusion of ions and other small molecules through the channel transfers the action potential in the postsynaptic cell. B) Gap junction channels are made up of gap junction proteins called Connexins. Six Connexins form hemi-channels on either side of a synapse, which can open and close to allow for controlled passage from neuron to neuron. C) Electrical synapses are the first to form during development. These early electrical synapses then mature into either persistent electrical synapses or chemical synapses as development continues and the neural networks continue to mature.

Neural circuit development is driven by genetics and activity during development

Prior to synapse formation, newborn neurons extend processes (axons and dendrites) into the space around them in a process called neurite guidance, which occurs

between the sixth and twenty-fourth weeks of development in humans (Figure 4, Anderson, 2003.). Intrinsic cell processes prompt the neuron to grow dendrites or axons in particular directions. Growth factors produced within the cell by particular gene expression can guide axons, modulate filopodial motility, and direct a neuron's growth cone. Additionally, extrinsic cues from ligands outside the cell can interact with receptors on a neuron's surface and cause a signaling cascade that can induce morphological changes in the axon growth cone (Shen & Cowan, 2010). Thus, a neuron's development is directed both by autonomous, intrinsic decisions and by non-autonomous, extrinsic cues sent by neighboring cells.

These intrinsic decisions are often directed by specific gene expression in certain cells. Gene expression depends on a number of mechanisms that modulate which genes are expressed in particular cells. Genes are housed in DNA, a molecular blueprint for protein synthesis. The central dogma of molecular biology describes how DNA base pair sequences are transcribed into RNA which is then translated into protein. Proteins provide the building blocks for creating and acting on cellular structures. Some of these proteins form synapses between neurons. The presence of different proteins can induce vastly different effects due to proteins' functional diversity. For example, proteins like Connexins, when expressed, can build or mediate synaptic activity between two neurons (Kandel et al., 2014).

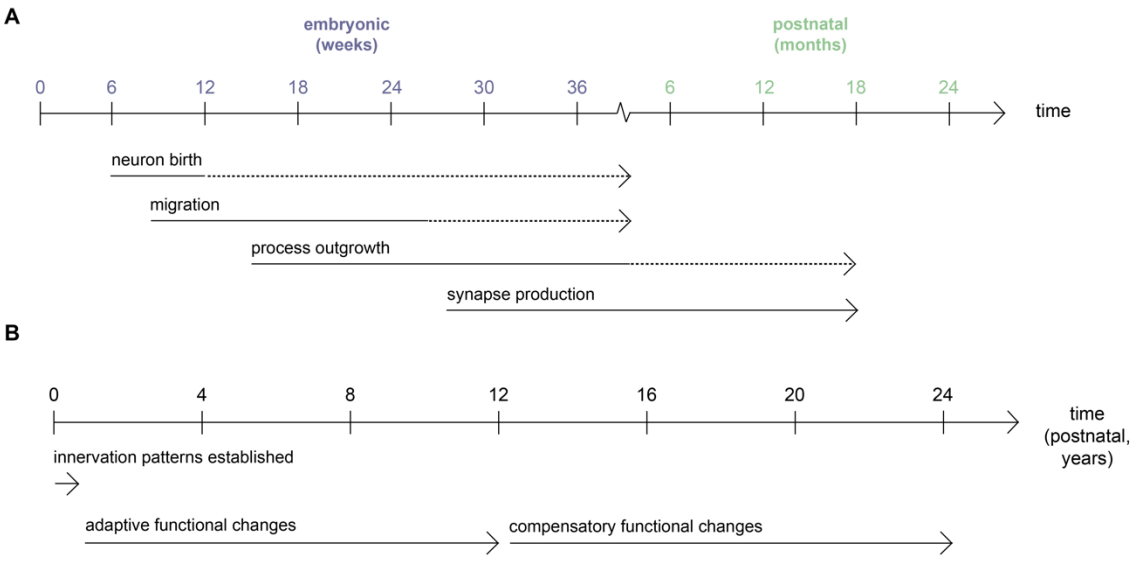

Figure 4. Stages of brain development.

A) Neurons begin to differentiate from **progenitor** cells six weeks into development. Soon after, the neurons migrate into their predetermined locations and project processes into the space around them Using internal and external cues, neurons decide which synapses to form with other neurons around them. Disruptions in early migration and connectivity due to problems in axonal or dendritic outgrowth or synapse formation result in changes to innervation patterns, resulting in altered formation of neural circuits. These changes can result in functional changes in brain activity. **B)** After innervation patterns are established, both adaptive and compensator changes in circuit formation begin to occur to accommodate the circuits established early on in development. Figure modified from Anderson, 2003.

After a neuron's processes are guided to its correct location, it finds other neuronal processes that it can choose to form a synapse with or not (target selection). Target selection is determined by a combination of chemoaffinity and locality that together direct neurons to form stabilized contact with other neurons. Similar to the processes that drive guidance, neural circuits are formed through two mechanisms, one intrinsic and one extrinsic. Extrinsic mechanisms include activity-based neural wiring, or Hebbian plasticity, which enhances the formation of functional circuits through

simultaneous neural activity (Martens et al., 2015). For example, connections between motorneurons and muscle cells, at neuromuscular junctions, form through a combination of interactions between motorneurons and muscle fibers. In addition to motorneurons secreting factors that are detected by muscle surface receptors to prompt synapse formation, the connections are also strengthened through synchronous activity between the neurons and corresponding muscle cells (Hoch, 1999).

Although activity-based mechanisms are at play in building neural networks, the initial steps of circuit formation must be driven by genetically-induced recognition events. Without the first genetically-based synapses and genes encoding proteins that build functional systems, early network formation would not be possible. Thus, genetics are the basis for early network formation.

The molecular basis for the first neuronal connections

Electrical synapses are hypothesized to be the first connections to form between neurons during development. Such early connections have been found widely in both invertebrate and vertebrate nervous systems (Saint Amant et al., 2001; Peinado et al., 1993; Nadarajah et al., 1997; Chang and Balice-Gordon, 2000; Roerig and Feller, 2000). Electrophysiology recordings of the first active neurons in the zebrafish spinal cord showed that upon addition of chemical synapse blockers, neural activity persisted. However, when embryos were exposed to the electrical synapse blocker heptanol, neural activity promptly ceased, indicating that the first active neurons wire together using electrical synapses. Early electrical synapses then develop into either more mature electrical or chemical synapses (Figure 3C, Hormuzdi et al., 2004, Saint Amat et al., 2001). For instance, when these synapses are inhibited for long periods of time,

synchronized circuits fail to form (Warp et al., 2012). Electrical synapses coordinate activity in the developing brain and provide important metabolic signaling that is critical for mature networks to form. Initial formation of these early electrical synapses is directed by genetics and other intrinsic cues, but the molecular composition of these first gap junctions are still unknown. The genes that encode these first Connexin proteins are a critical gap in our knowledge.

Research Aims

The goal of this thesis was to identify Connexin proteins required for the first synapses formed during vertebrate nervous system wiring. To achieve this we needed an accessible model system in which initial electrical synapse formation could be monitored as well as a system in which we could manipulate genes to affect behavior. To this end, we used the first spinal cord circuits that wire together in zebrafish (*Danio rerio)*. Zebrafish possess several benefits as a model organism for this project. Their genome contains homologs for 70% of human protein-coding genes and 84% of genes associated with human disease, making them suitable for human-related studies (Howe et al. 2013). Additionally, modern techniques in molecular genetics have made gene knock out possible. Zebrafish are also advantageous because they are bred with relative ease, laying large quantities of eggs that develop externally, providing easy access to the developing nervous system. For this study, the zebrafish spinal cord served as the model neural circuit, as spinal cord neurons and their development have been well characterized, offering more clarity into molecular processes while still mirroring increasing complexity that occurs during brain development.

The early spinal cord circuit is the precursor of the central pattern generator (CPG) that allows for rhythmic motor behaviors, like beat-and-glide swimming (Figure 5). CPGs are a type of neural network that produces repetitive motions such as walking or breathing. Juvenile and adult zebrafish swim rhythmically without rhythmic input from the brain, a hallmark feature of CPGs (Marder and Bucher, 2001). This sophisticated and controlled swim circuit arises throughout development and begins with spontaneous coiling behavior 17 hours into development (hours post fertilization, or hpf). During the initiation and first hours of coiling, interneurons and motorneurons are coupled via electrical synapses, first in local groups within a segment, then spreading to connect the segments into larger, coordinated functional groups. Zebrafish have 30 repeating spinal cord segments whose neurons eventually link together, connecting the segments into a single network throughout the entire spinal cord (Warp et al., 2012). Neurons involved in coiling have been previously characterized to include the three primary motorneurons (rostral primary (RoP), middle primary (MiP), and caudal primary (CaP)), as well as ventral ipsilateral (same side) descending (VeLD) and ipsilateral caudally projecting (IC) interneurons. Contralaterally (opposite side) extending interneurons such as commissural primary ascending (CoPA) and commissural secondary ascending (CoSA) neurons also become involved in coiling, although slightly later in development (Saint Amant et al., 2001, Figure 5C).

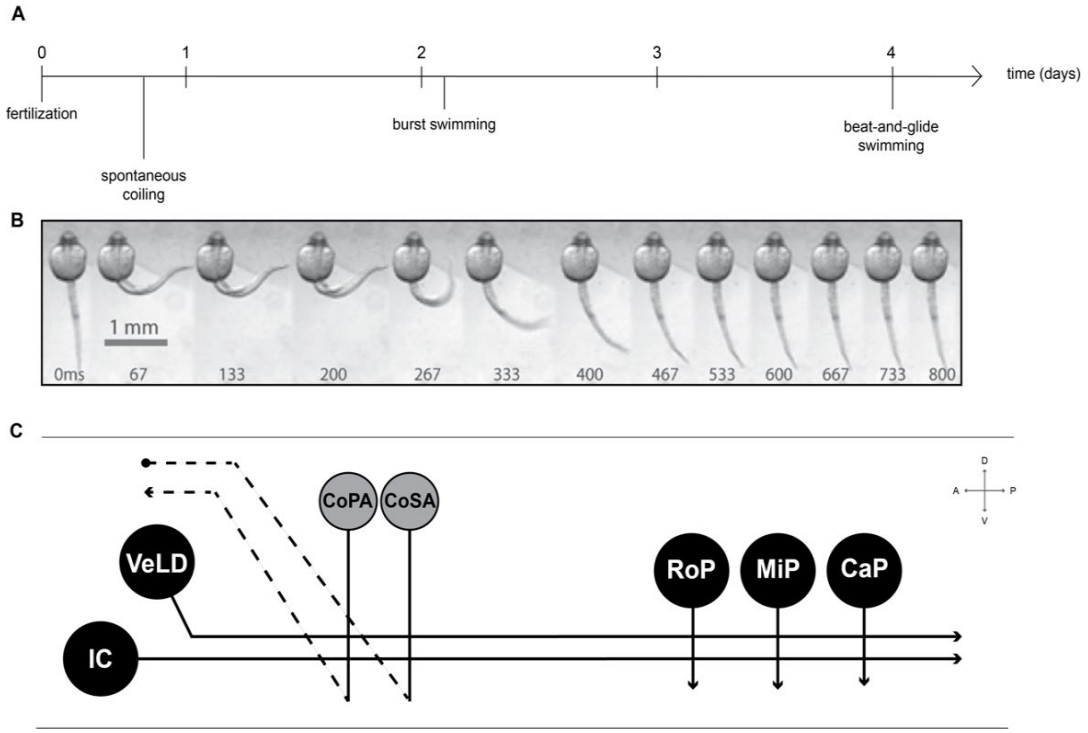

Figure 5. Central pattern generators and complex motor behaviors develop over time.

A) The central pattern generator that gives rise to complex behaviors like beat-and-glide swimming develop sequentially. The process begins with spontaneous coiling, a simple behavior that arises 17 hpf. Coiling is the first evident behavior during development and precedes the development of the embryo's sensory system and voluntary control. Timeline modified from Drapeau et al., 2002. B) Sequence of a coil in a 26 hpf embryo. Still images taken at 67 ms intervals from a video recording of an agarose-embedded fish. Modified from Knogler et. al, 2014. C) A simplified spinal circuit in a single segment of the early spinal cord. Neurons involved in spontaneous coiling behavior from the initiation are IC and VeLD interneurons and RoP, MiP, and CaP motorneurons (black). CoPA and CoSA interneurons, which travel contralaterally (dashed line) to link left and right sides, are believed to become involved in coiling around 20 hpf (grey). Anterior is to the left, ventral is below. Figure modified from Saint Amant et al., 2001.

Because spontaneous coiling, the first behavior that zebrafish exhibit during development, is facilitated by neurons connected via electrical synapses, we used coiling as a behavioral indicator for coupled circuits. We hypothesized that eliminating a Connexin critical to early electrical synapse formation would also disrupt behavior between 17 and 24 hpf. Because early spinal cord circuits are electrically coupled, Connexins are the most probable molecules that build gap junction channels between these neurons. We therefore used behavior of zebrafish with missing proteins to infer where and how the corresponding Connexin proteins might be localized and functioning. For example, complete paralysis of an animal lacking a particular gene may indicate that the encoded Connexin protein might couple motorneurons with interneurons and, without these connections, information to contract or relax muscle is not transmitted.

Results

Identification of potential electrical synapse *connexins* expressed within the early developing zebrafish spinal cord

As a first step towards identifying Connexins that might be acting in the spinal cord early in development, we examined the family of *connexin* genes encoded in the zebrafish genome. We used information about the known human *connexin* genes (20 genes) and examined the evolutionary relationships amongst these genes within the zebrafish genome. We identified 45 genes encoding potential Connexin proteins in the genome. To identify which of these genes might be important to coiling behavior and its underlying circuits we wanted to identify those that were expressed in 20 hpf zebrafish spinal cord neurons. To achieve this we examined the expression of genes within primary motorneurons and VeLD neurons by isolating those cells and then subjecting them to RNA-sequencing analysis. These experiments were performed in collaboration with Drew Friedmann and Ehud Isacoff at the University of California, Berkeley. Results from Friedmann's RNA-sequencing dataset identified five electrical synapse genes that were enriched in spinal cord neurons. The neurons were isolated using the *1020:Gal4* enhancer trap transgenic line with the calcium indicator GCaMP5. In this line, ventral precursor neurons including primary motorneurons (PMNs) and VeLDs, two of the four earliest active cell types, were illuminated by GCaMP5s because of an insertion near ***olig2*** (Saint-Amant et al., 2001). These illuminated neurons were sorted from the unilluminated neurons using fluorescent-activated cell sorting (FACS) and the RNA present in those cells were sequenced and quantified for gene expression. The

gene expression levels from the *1020:Gal4* subpopulation of neurons were compared to those from the pan-neuronal *HuC:Gal4* line, in which all neurons were illuminated. This control allowed us to compare the subset of neurons known to be involved in early circuit formation with all neurons.

Five electrical synapse genes/Connexin proteins were expressed in ventral neurons illuminated by the *1020:Gal4+* line. *gjd1a/*Cx34.1*, gjd2b*/Cx35.1, and *gjd2a*/Cx35.5 were expressed in ventral neurons (Figure 6A, Table 1, Shah et al., 2015). *gjc2*/Cx43.3 showed extremely high expression relative to the other genes in ventral neurons as well. This Connexin is known to be broadly expressed throughout the entire body, including in neurons (Table 1, Landesman et al., 2003). *gjd4*/Cx46.8 was also expressed in the *1020:Gal4+* line. Very little is known about when and where this gene acts in the spinal cord.

Once we identified which genes were expressed in neurons involved in coiling, we analyzed the data for which genes are upregulated in ventral neurons compared to *HuC:Gal4+* neurons. *gjd1a/*Cx34.1*, gjd2b*/Cx35.1, and *gjd2a*/Cx35.5 showed elevated levels in the *1020:Gal4+* line as did *gjd4*/Cx46.8 (Figure 6B). By contrast, *gjc2*/Cx43.3 showed elevated expression levels in the *HuC:Gal4+* line. We chose to include it as a candidate Connexin because of its extremely high expression levels in ventral neurons.

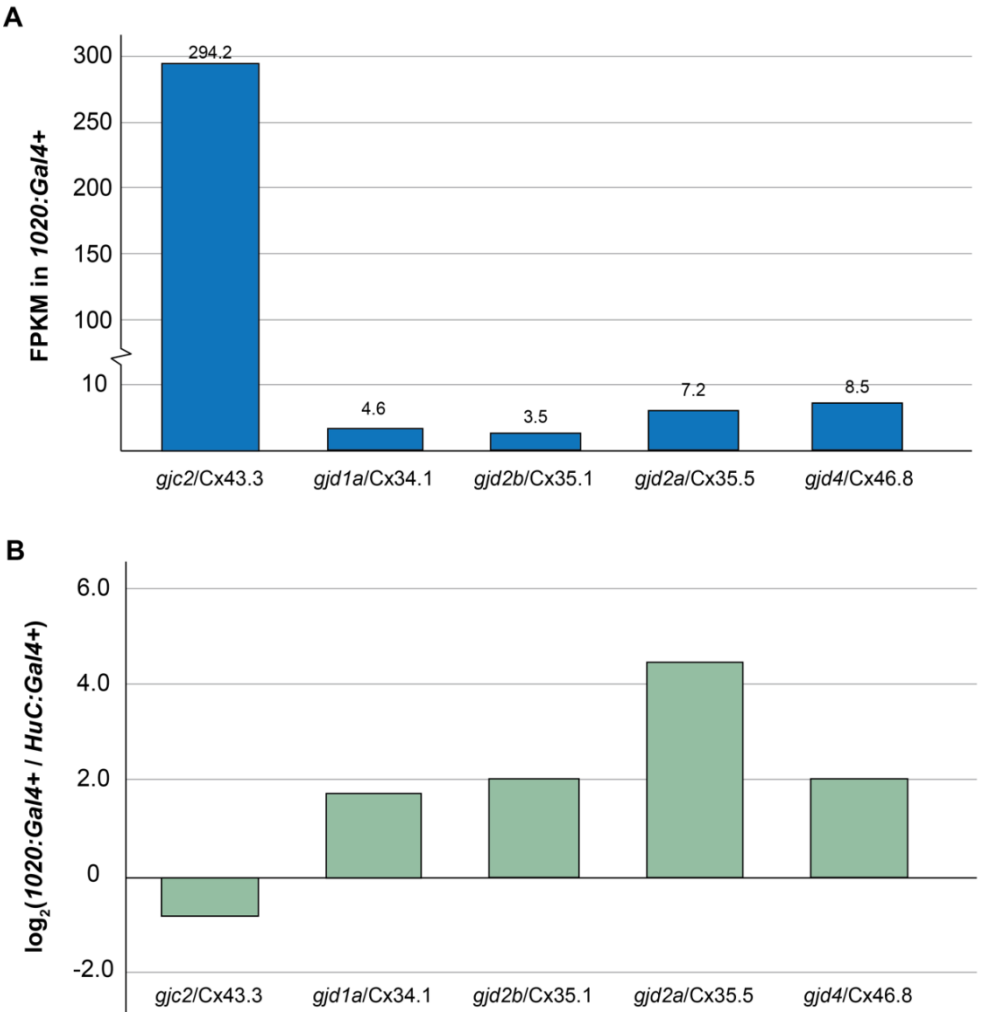

Figure 6. RNA-seq results suggested five genes-of-interest.

A) Expression levels (quantified by fragments per kilobase of transcript per million mapped reads) in *1020:Gal4+* line alone. Although *gjc2*/Cx43.4 was preferentially expressed in all neurons rather than our subset, its high expression levels identified it as a gene-of-interest as well. B) Each gene expression level in *1020:Gal4+* was normalized to the expression levels of all neurons, represented by *HuC:Gal4+*. Positive values indicate higher expression in *1020:Gal4+* ventral neurons involved in coiling. Negative values represent higher expression in *HuC:Gal4+* neurons. *gjd1a*/Cx34.1, *gjd2b*/Cx35.1, *gjd2a*/Cx35.5, and *gjd4*/Cx46.8 all show elevated expression levels in the *1020:Gal4+* subset of neurons, while *gjc2*/Cx43.4 showed elevated levels in the *HuC:Gal4+* line.

In humans, Cx36 is thought to be the predominant neuronal Connexin, and *gjd1a*/Cx34.1, *gjd2b*/Cx35.1, and *gjd2a*/Cx35.5 are all zebrafish orthologues of this gene (Table 1, Shah et al., 2015). *gjd1b*/Cx34.7, the fourth gene in the *Cx36* family, was absent from the dataset. However, because all other *Cx36* family genes were expressed at elevated levels in this neuronal subset, we included *gjd1b*/Cx34.7 as a candidate *connexin*.

Table 1. Electrical synapse genes-of-interest and current knowledge of their localization and function.

gene-of-interest	protein	current understanding of expression & function
gjd4	Cx46.8	None
gjc2	Cx43.4	Compensates for lack of expression of Cx45 in muscle formation/regeneration in mice (von Maltzahn et al., 2006), widely expressed in muscle throughout body, also present in brain and eyes in *Xenopus* embryos (Landesman et al., 2003), necessary for generation of asymmetric signals across left-right axis for internal organ function (Hatler et al., 2009).
gjd1a	Cx34.1	*Cx36* orthologue, necessary for synapses between the Mauthner and commissural local (CoLo) neurons involved in zebrafish escape response (Shah et al., 2015).
gjd1b	Cx34.7	*Cx36* orthologue, necessary for synapses between auditory afferents and Mauthner and CoLo neurons in goldfish (Rash et al., 2013).
gjd2b	Cx35.1	*Cx36* orthologue, highly expressed in retina (McLachlan et al., 2003), necessary for synapses between auditory afferents and Mauthner and CoLo neurons in goldfish (Rash et al., 2013).
gjd2a	Cx35.5	*Cx36* orthologue, necessary for synapses between the Mauthner and CoLo involved in zebrafish escape response (Shah et al., 2015).

Knock out of *connexin* gene function using the CRISPR/Cas9 system

After identifying the electrical synapse Connexins that are expressed in the neurons involved in coiling, we proceeded to create zebrafish lacking those specific proteins. Without those Connexin proteins, the electrical synapse formation underlying

neural circuits involved in coiling behavior may be disrupted, allowing us to identify which Connexins are important for the system. We created deletions in our electrical synapse genes-of-interest using Clustered Regularly Interspaced Repeats (CRISPR)/Cas9 targeted genome editing. This technique sends Cas9 enzyme to cleave DNA at specific sites. Guided by a strand of RNA complementary for the target gene, Cas9 cuts the DNA at a specific locus. We used this technique to knock out Connexin function.

After we used CRISPR/Cas9 genome editing to induce mutations in electrical synapse genes, I sequenced the targeted genes to find mutations. A mutation can be the deletion of an entire gene or a modification. Sequencing analysis showed that CRISPR/Cas9 caused an 8 base pair (bp) deletion in *gjd4/*Cx46.8 at the beginning of the second exon (Figure 7A, C). Because protein structures are defined by groups of amino acids encoded in base pair triads, a deletion of 8 base pairs results in the loss of several amino acids but more importantly shifts the triads over, resulting in a **frameshift mutation** that is likely to knock out the remaining protein structure or produce a deformed, nonfunctional protein. Results from the reverse transcription-PCR experiment, a technique used to find whether a gene is actively transcribed, supported the idea that the identified 8 base pair deletion resulted in the loss of the entire gene (Figure 7E). Although transcription level in control animals with non-mutated copies of *gjd4/*Cx46.8 is already low, apparent levels in *gjd4/*Cx46.8 mutant animals are still more depleted. *Beta actin 2* (*bact2)*, a gene expressed in muscle, and *eukaryotic translation elongation factor 1 alpha 1, like 1* (*eef1a1l1)* were used as a control and show comparable levels of transcription in both control and *gjd4/*Cx46.8-/- animals.

In *gjc2*/Cx43.4, sequencing revealed a 4 bp mutation in the second exon of the gene at the CRISPR target site (Figure 7B, D). A mutation of this size would also induce a frame shift in the genome and would be expected to produce a non-functional protein. Confirmation of loss of RNA, as done with *gjd4/*Cx46.8, is in progress. Mutations in *gjd1a*/Cx34.1, *gjd1b*/Cx34.7, *gjd2a*/Cx35.5, and *gjd2b*/Cx35.1 were generated previously by the Miller lab (Miller et al., 2017).

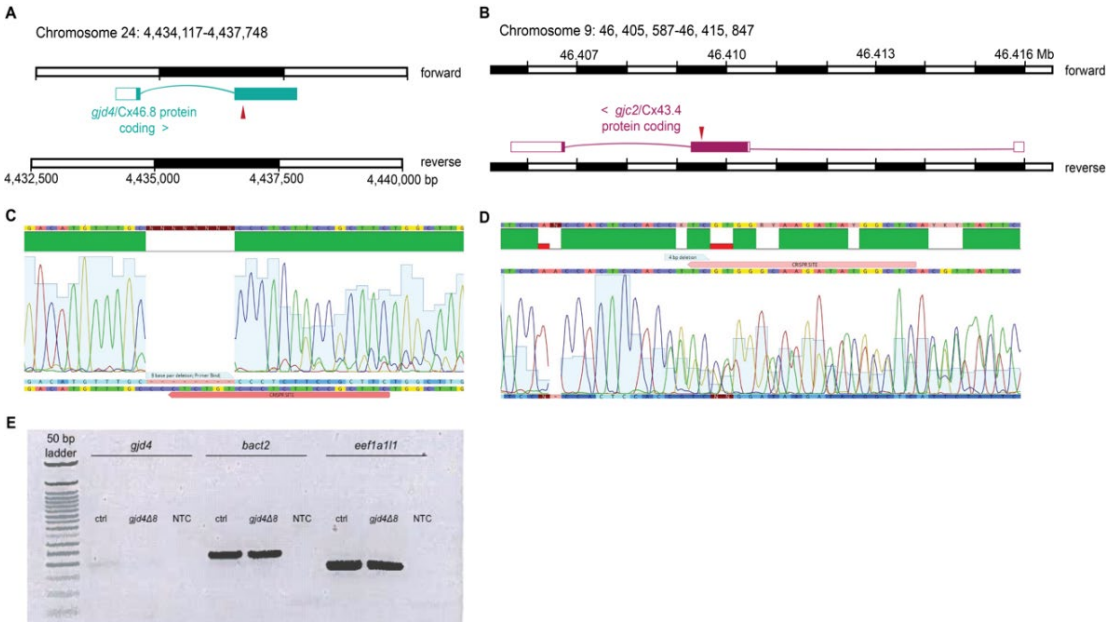

Figure 7. Genotyping results show frame shift mutations in both *gjd4*/Cx46.8 and *gjc2*/Cx43.4.

A-B) Locations of both *gjd4*/Cx46.8 and *gjc2*/Cx43.4. *gjd4*/Cx46.8 spans two exons on Chromosome 24 and *gjc2*/Cx43.4 spans three exons on Chromosome 9. CRISPR/Cas9 target sites for both genes were at the beginning of exon 2 (denoted with red carrot). C) CRISPR/Cas9 editing produced an 8 bp deletion at the CRISPR site in *gjd4*/Cx46.8. Sequencing results pictured here were derived from DNA from an animal homozygous for this deletion. D) CRISPR/Cas9 editing produced a 4 bp deletion at the CRISPR site in *gjc2*/Cx43.4. Sequencing results pictured here were derived from DNA from an animal heterozygous for this deletion, which is why following the deletion there are two main peaks shown for each trace file. E) Reverse transcription-PCR results showing that while *gjd4*/Cx46.8 expression levels are already low in control animals that do not carry the 8 bp deletion, mutants for this gene produced even lower levels. The control experiments for *bact2* and *eef1a1l1* show that there is no difference in gene expression in other genes between control and *gjd4*/Cx46.8 mutant animals.

Quantitative behavioral analysis to examine coiling behavior

Following genetic knock out of the *connexins*, we set about observing the effect of their loss on coiling behavior. To do so required developing a methodology that imaged and quantified coiling in a way that we could then understand the similarities and differences between control and mutant behavior.

I tried several strategies to efficiently orient the fish to visualize their tail motions. I first developed an agarose mold that created small teardrop-shaped indentations with dimensions of 1500 µm x 750 µm at the widest point and a depth of 300 µm. These dimensions were based on the approximate dimensions of a 20 hpf zebrafish. The indentations had a rounded bottom, intended to hold the dorsal region of the zebrafish in place while the tail was free to extend from the well and move without disruption (Figure 8A). The agarose mold was drafted using AutoDesk and manufactured by the UO Machine Shop. The mold was then floated on 2% agarose in a petri dish until the agar solidified. With this method, we could quickly mount 42 embryos on one agarose plate. However, although the embryos were easy to place into the wells, they were not always contained in them throughout the duration of imaging. As their coils became stronger, particularly around 22 hpf in control fish, their vigorous movements lifted them out of the wells and away from our imaging setup. Additionally, because the embryos escaped the wells during imaging we were unable to track individual fish throughout development.

We then decided to embed the embryos in 1.8% low-melt agarose in embryo medium to hold them in place. Each embryo was embedded in a droplet of agarose, oriented with their dorsal surface resting against the bottom of a petri dish. I would then flood the plate with embryo medium and clear agarose away from the tail allowing for full range of motion of the tail, leaving only the head and part of the yolk sac embedded in the agar (Figure 8B). With this method, I was able to perform long-term imaging on fish that could not move away from their positions, but with free range of motion for their tails. Although this setup was more time consuming during initial mounting than

with the agarose mold, it proved more sustainable for long-term imaging and provided us with consistent body orientations and images for analysis.

To capture images of behavior across time, I worked with Sarah Stednitz, a PhD student in the Washbourne lab at University of Oregon. We went through several iterations of cameras, lenses, light sources, and software to optimize image contrast between the transparent fish body and the surrounding agarose and embryo medium. The clearest contrast was achieved by imaging from below the petri dish, with a light source illuminating the embryos from above (Figure 8C-E).

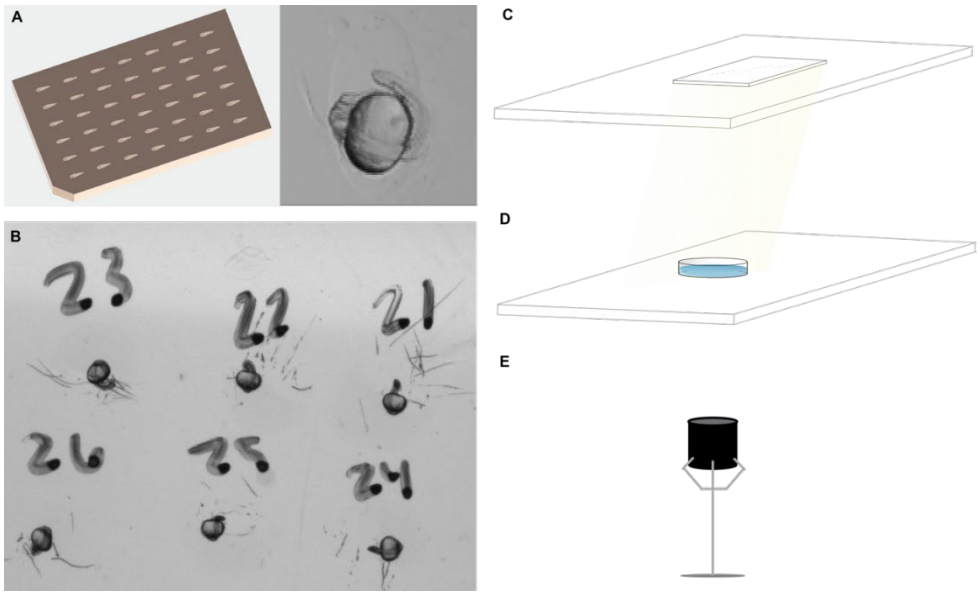

Figure 8. Behavioral imaging setup.

A) Agarose mold with teardrop shaped ridges that form indentations when floated in 2% agarose. 23 hpf embryo in coiling a well. B) Agarose mounted fish (18 hpf) with tails cleared for motion, labeled with fish ID numbers. C) A 6.5"x6.5" light panel was suspended on a transparent plastic sheet for illumination. D) The petri dish containing the agarose-mounted embryos was suspended on another transparent plastic sheet. E) A high-speed 5MP Monochrome CMOS Camera imaged the embryos' behavior from below to optimize how visible the transparent, day-old embryos were in the petri dishes.

To analyze coiling behavior, Stednitz created a program in Python that preprocessed the image sequences for analysis. The program first screened through the full image sequence and subtracted unchanging elements of the images – in this case, the background agar and embryo medium and unmoving upper body of the fish were eliminated and only the tail's motion was retained, making tracking the tail easier. Stednitz then manually defined the top and bottom of the fish's tail. The program could then detect tail contour and motion, outputting coordinates of the tail's trajectory during each coiling event (Figure 9) I used these coordinates to analyze coiling frequency and strength, measured by angle of coils.

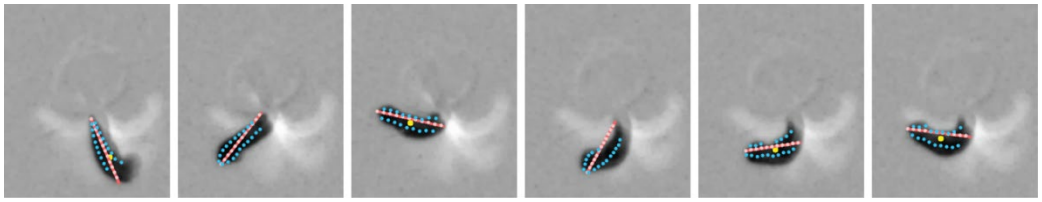

Figure 9. Image sequence preprocessing subtracts background to help isolate tail movements.

The red line drawn down the length of the tail tracks distance from the manually defined top point and the detected tail point (blue) furthest from the top. Yellow point is center of mass.

*gjd4/*Cx46.8 is required for coiling behavior performance

We analyzed control fish behavior to characterize how normal coiling behavior emerges between 18 and 24 hpf. *zf206ET* (control) animals typically began moving their tails at 17 hpf. With each passing hour the movements of the tail became stronger (i.e. more "deliberate") and more pronounced in curvature, measured by the angle from rest (tail laying straight from head).

After characterizing control behavior we analyzed each Connexin mutant's behavior to see any visible changes. Cx35.1, *gjd1a*/Cx34.1, *gjd2a*/Cx35.5, and *gjd1b*/Cx34.7, the Cx36 family, showed no overt changes in coiling between 18 and 24 hpf. Because of the possibility of genetic redundancy among these four genes, we created lines of zebrafish carrying mutations in all of the Cx36 family genes. These quadruple mutant fish also showed no change in coiling behavior other than a slight delay in onset (Figure 10). However, this was accounted for by developmental delays

characteristic of mutant animals. Similarly, *gjc2*/Cx43.4 showed no visible change in coiling.

Disrupted coiling appeared in *gjd4*/Cx46.8 mutant fish. One potential effect of electrical synapse loss might have been a change in coiling frequency between control and mutant fish. I calculated the frequency of coils measured in movements per minute across a five-minute period of imaging. Collapsing this data across animals showed that following coiling initiation, *gjd4*/Cx46.8 mutant animals attempted to coil just as frequently as control fish between 18 and 24 hpf (Figure 10).

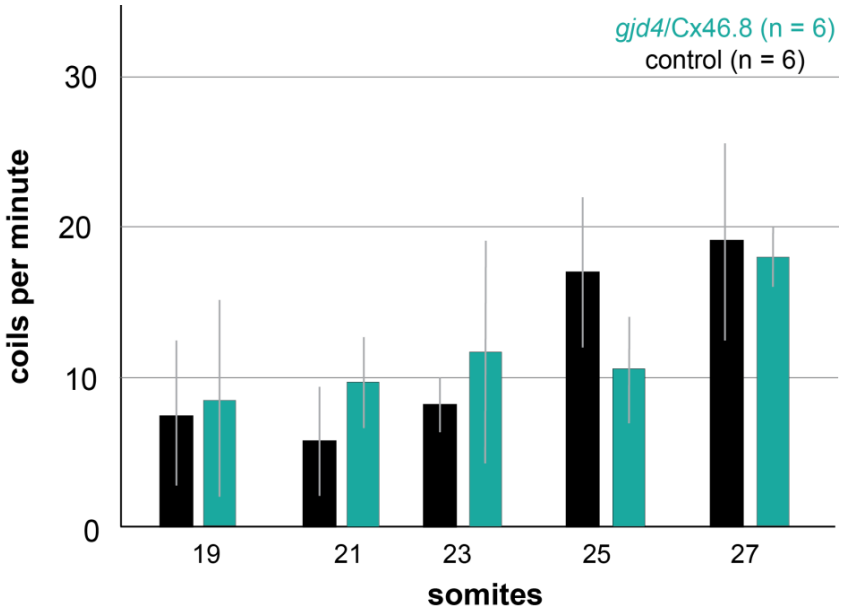

Figure 10. Coiling frequency is not different between control fish and *gjd4*/Cx46.8-/-.

Once coiling is initiated in *gjd4*/Cx46.8 mutant fish, they attempt to coil just as frequently as control fish. Coiling frequency in control fish is also highly variable across individuals, particularly in 24 hpf embryos.

Several other changes in behavior were apparent in these Connexin knock out fish. First, the onset of coiling was delayed. Control fish initiated coiling at 17 hpf, at

approximately the 18 somite stage of development (Figure 11). *gjd4*/Cx46.8 mutant fish began between 19 and 20 hours in development. After correcting for developmental delays in mutant fish, we found that coiling initiation began between the 19 and 20 somite stage of development. This suggests that the absence of *gjd4*/Cx46.8 somehow causes synapse formation in spinal circuits involved in coiling to be delayed.

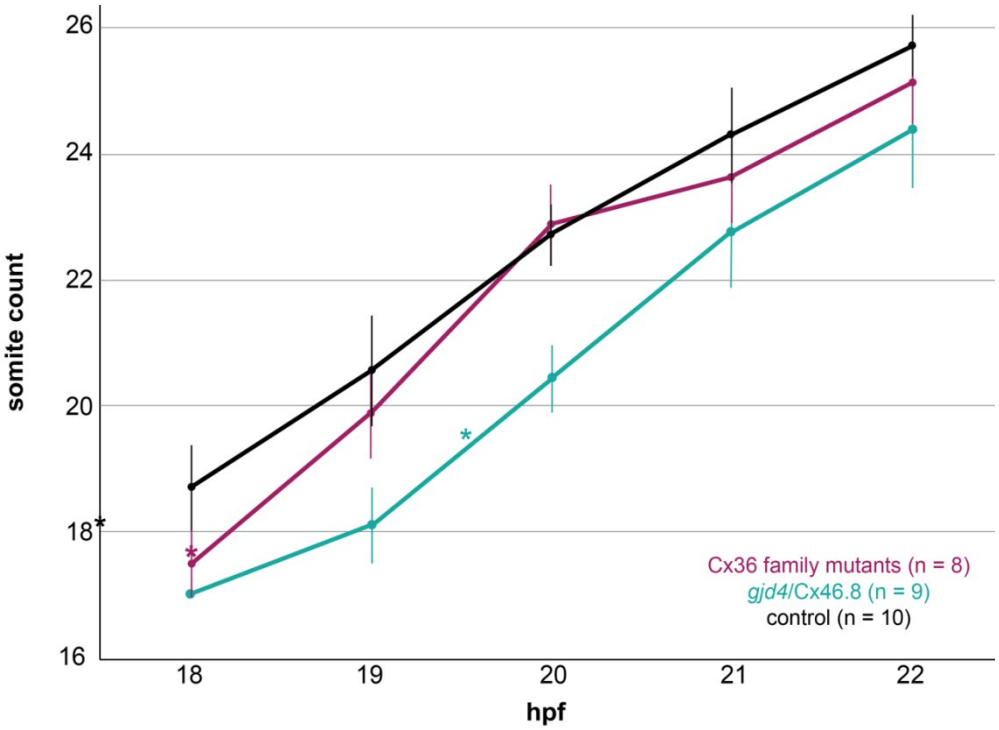

Figure 11. Mutant animals are developmentally delayed.

Control fish begin coiling at 17 hpf (indicated by asterisk). *Cx36* family mutants (carrying mutations in all 4 family members) are developmentally delayed. However, when somite count is aligned between *Cx36* mutants and control fish, onset of coiling begins at roughly the same developmental stage. By contrast, *gjd4*/Cx46.8 mutant fish are both developmentally delayed and have delays in coiling onset, even after correcting for somite count. Error bars represent standard deviation.

The second apparent phenotype in *gjd4*/Cx46.8 knock out mutants was a decrease in coiling strength (measured by trunk angle) on either side of the animal.

After correcting for developmental age, I measured the trunk angles at the peak of a coil event on either side of the body for each stage. Between 19 and 31 somite stages, the decreased trunk angle observed *gjd4*/Cx46.8 mutants as compared to control fish was statistically significant ($p<0.0001$, Figure 12). This result represents a dramatic decrease in coiling behavior strength in *gjd4*/Cx46.8 mutants, suggested in a change in synaptic strength in the underlying neural circuits.

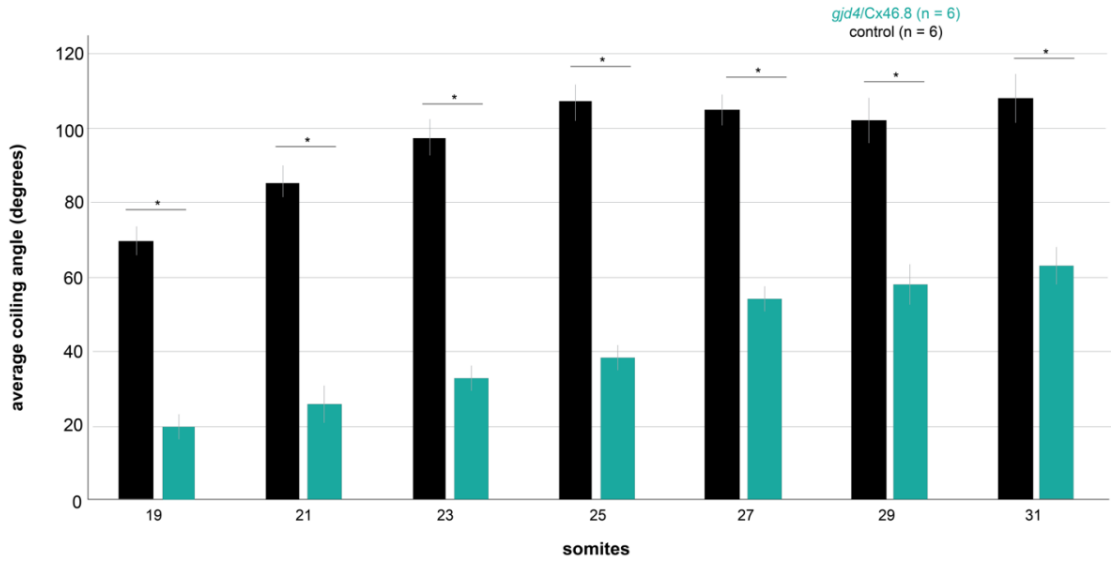

Figure 12. Coiling strength in *gjd4*/Cx46.8 mutant animals is significantly decreased between the 19 and 31 somite stages.

The peak of the coil, measured in angles from rest, was calculated for each coiling event and collapsed across left and right sides for each animal. Control animals show a significantly greater range of motion and coiling strength for every time point between 19 and 31 somites ($p<0.0001$, unpaired two-tailed t-test). Error bars represent standard error.

The third change in phenotype was a consistent asymmetry in coiling strength between the left and right sides of the fish's body. Mutant fish had a strong and weak side of coiling which could either be the left or right side (Figure 13). Throughout development between 19 and 31 somite stages, coiling strength on each side would

increase but one side would remain stronger compared with the other. However, coiling strength/preferred side could change throughout development in a single animal – for example, an animal with a stronger left side at coiling initiation could switch to having a stronger right side at 25 somites and maintain that strength throughout the remaining experiment duration. When our data was collapsed across all time points and the difference between strong and weak sides were taken, the difference in control and *gjd4*/Cx46.8 behavior was significant ($p<0.0001$, Figure 14). This might suggest that neurons driving contralateral control may be affected by the Connexin protein's absence. The inability to properly initiate a bend to the opposite side may be due to the left and right sides' lack of communication – in control animals when one side of the spinal cord is active, the other side is inhibited for the duration of the coil. When the coil is complete, inhibition is lifted and the contralateral side is permitted to activate (Warp et al., 2012). The asymmetry in *gjd4*/Cx46.8 mutant fish may be due to an absence of this contralateral connection.

Figure 13. *gjd4*/Cx46.8 mutant fish display asymmetry in coiling strength.

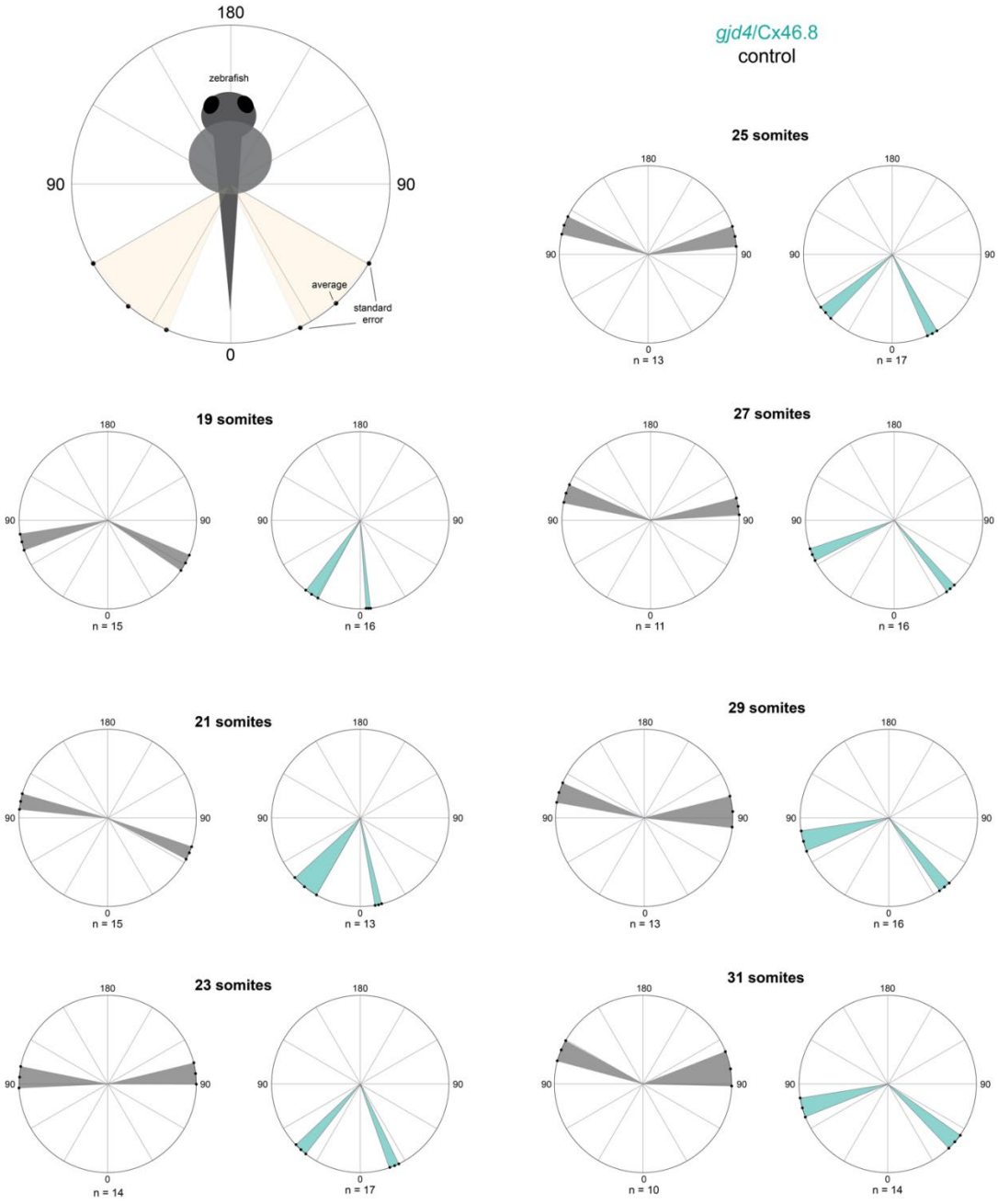

Average coiling angle, measured by the maximum angle achieved during each coil's inflection, across time. Angle was measured from rest, as shown in the top left figure. The left coils of control animals are represented by the left side of their plots while the right coils are represented by the right side of the plots. *gjd4*/Cx46.8 angles were classified by "strong side" (left side of plots) and "weak side" (right side of graphs) rather than by physical left and right sides. For each plot, the center point represents average and exterior points represent standard error.

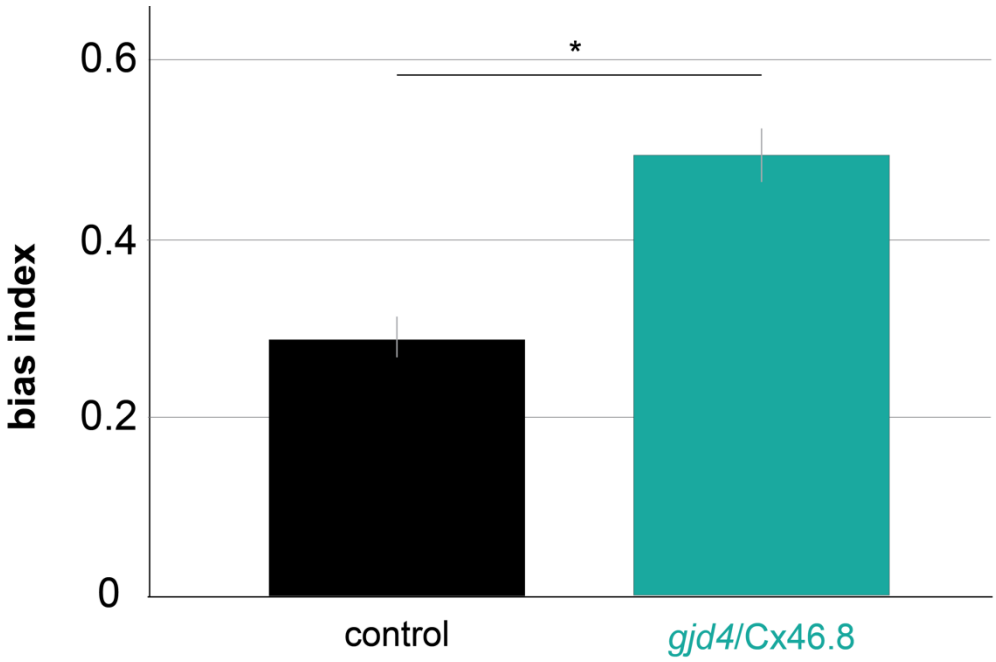

Figure 14. Difference in coiling strength between strong and weak sides.

Sides were classified as "strong" and "weak" for both control and *gjd4/*Cx46.8 animals. To calculate bias, the difference in peak trunk angle was taken between the "strong" and "weak" sides, then divided by the overall angle of the "strong" side. The difference was statistically significant ($p < 0.0001$, unpaired two-tailed t-test).

Discussion

The purpose of this thesis was to identify Connexins involved in early electrical synapse formation that couple the first neural circuits in the zebrafish spinal cord. We identified a connexin gene/protein, *gjd4*/Cx46.8, that was present in the spinal cord at 20 hpf and whose absence provoked visible changes in coiling behavior. Behavior arises from neural circuits and, in the early zebrafish spinal cord, these circuits are linked together by electrical synapses. Because Connexins are a key protein at electrical synapses, we had hypothesized that the presence of Connexins in these early circuits are the molecular basis for coiling behavior. Our results suggest that *gjd4*/Cx46.8 is involved in building electrical synapses in early forming circuits. We observed a delay in coiling initiation in these mutants, as well as an overall decrease in coiling strength. These results imply an initial absence of usual synaptic communication that then evolves into decreased synaptic strength. The mutant fish also exhibited asymmetry in coiling strength between the left and right sides of the body, suggesting that contralateral coordination neurons are disrupted by *gjd4*/Cx46.8 absence. Further work is necessary to understand how *gjd4*/Cx46.8 is involved in circuit function and development.

Future Directions

While we have identified a behavioral defect, the immediate next steps of this project are to find where *gjd4*/Cx46.8 gene and protein is expressed and localized. Ongoing experiments are in progress to perform RNA in situ hybridizations with targeted probes to visualize where *gjd4*/Cx46.8n messenger RNA (mRNA) is transcribed within the spinal cord. I have already synthesized an RNA probe that is complementary to transcribed *gjd4*/Cx46.8 RNA labeled with digoxigenin. This will label *gjd4*/Cx46.8 mRNA transcripts and allow us to identify the cells that Cx46.8 is expressed. I am currently optimizing colorimetric RNA in situ hybridization protocols for our probes and for fish at 24 hpf. We also plan to generate an antibody against Cx46.8 protein to help us visualize localization of the protein within early neural circuits. We hypothesize that Cx46.8 is localized at synapses between neurons involved in the coiling circuit.

We will then aim to better understand early circuit dynamics involved in constructing the first functional networks in the spinal cord and how these dynamics are changed in our *gjd4*/Cx46.8 mutant animals. To do so, we have partnered with Philipp Keller's lab at Janelia Research Campus. Yinan Wan, who works in the Keller lab, has performed calcium imaging across entire segments of the spinal cord between 17 and 24 hpf to visualize circuit dynamics and understand the steps taken by different types of neurons to connect with one another. She has determined that primary motorneurons are the first to connect with neighboring neurons, and connect with other local neurons in a stepwise manner to form functional communities. Throughout development, these clusters of synchronized neurons expand between the segments of the spinal cord,

gradually forming larger communities through synchronizing inputs and increased neural connections. These communities within segments are then able to link together across segment boundaries and form fully synchronized networks up and down the spinal cord. The final step in network development is to link commissural interneurons that carry information contralaterally to link together the left and right sides of the body (Wan et al., personal communication).

Our next steps are to image the circuit dynamics in *gjd4/*Cx46.8 mutant animals to examine the effects on connectivity compared with the stereotyped emergence of coordinated spinal circuitry. If our hypothesis that *gjd4/*Cx46.8 acts on ipsilateral connectivity-driving primary motorneurons is correct, we would expect changes in the initial steps of ipsilateral functional community establishment. However, if *gjd4/*Cx46.8 is connecting contralateral neurons, we would expect disruptions in the final step for network formation, where commissural interneurons are linking together the two sides of the body.

Conclusion

The purpose of this thesis was to identify Connexins involved in the first synapses formed during vertebrate nervous system wiring. We used spontaneous coiling, the first behavior exhibited during zebrafish development, as an indicator for whether the neural circuits in the spinal cord were appropriately coupled. We have identified a gene, *gjd4/*Cx46.8, that when mutated produces a changed coiling phenotype in young zebrafish. The phenotype suggests problems in synaptic development and strength or in contralateral connectivity. However, further work must be done to determine where and how *gjd4/*Cx46.8 acts in the spinal cord to produce electrical synapses. Our results suggest that although we do not yet know where *gjd4/*Cx46.8 is acting, it is a gene that is required for proper synapse formation and early circuit formation.

Detailed Methods

Animal use and care

All experiments involving zebrafish were conducted following standard protocols and procedures set forth by the University of Oregon Institutional Animal Care and Use Committee. Fish were maintained using previously described protocols (Westerfield, 2007) in the University of Oregon zebrafish facility. Control lines (*zf206ET*) and *gjd4*/Cx46.8 mutants were light-cycle shifted 5 hours, with embryos born at 2 pm and analysis beginning at 8 am (18 hpf) and extending to 2 pm (24 hpf). *Cx36* family and *gjc2*/Cx43.4 lines were not light-cycle shifted, their embryos born at 9 am and behavioral analysis taking place from 3 am (18 hpf) through 9 am (24 hpf).

FACS & RNA-seq to identify genes of interest

Drew Friedmann, formerly of the Isacoff lab at University of California, Berkeley, performed all RNA-sequencing experiments and set up a collaboration with the Miller lab for data analysis (Figure 15). We reasoned that to find the Connexins responsible for the initiation of coiling behavior, we should identify those genes upregulated in neurons involved in coiling and compare them to uninvolved neurons To do this, Friedmann used fluorescent activated cell sorting (FACS) to isolate ventral precursor neurons, including PMNs and VeLDs, two of the four active cell types involved in coiling behavior (Saint-Amant et al., 2001). He combined either the *1020:Gal4* enhancer trap transgenic line, which expresses in PMNs and VeLDs because of an insertion near the *olig2* gene, or the *HuC:Gal4* transgenic line, which expresses in all neurons, with the Tg(UAS:GCaMP5) line, resulting in the expression of the

fluorescent molecule GCaMP5 in the neurons of interest (*1020*+) or all neurons (*HuC*+). Cells from each experimental condition (*1020*+ and *HuC*+) were separately dissociated and FAC sorted to isolate the fluorescent-positive cells. The UC Berkeley Genomics facility then prepped each sample for bulk RNA-sequencing. The gene expression levels from the *1020:Gal4+* subpopulation of neurons were compared to those from the pan-neuronal *HuC*+ line using the standard bioinformatics pipeline TopHat (Friedmann et al., 2015). The top 300 genes, ranked by significantly different expression levels, were selected for further analysis.

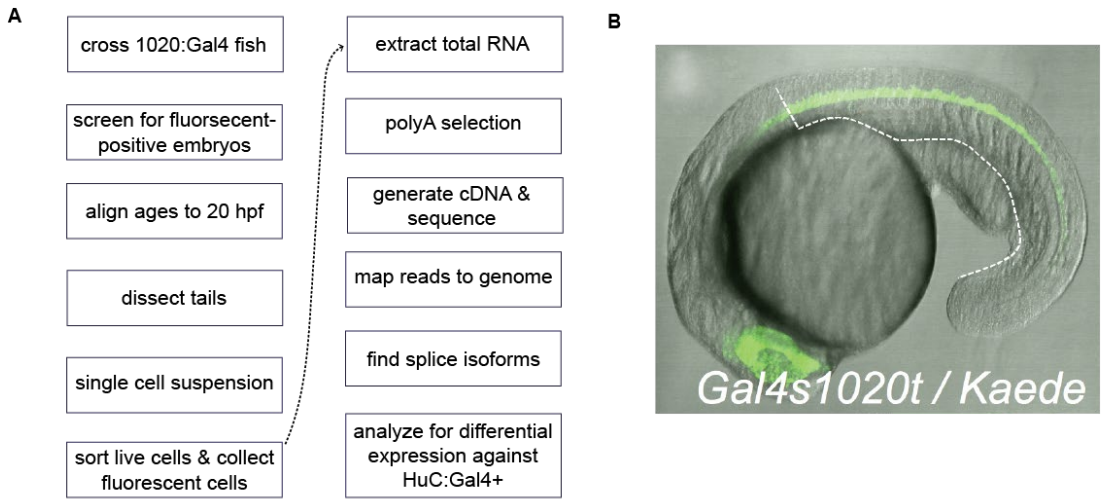

Figure 15. FACS & RNA-sequencing workflow.

A) Workflow for FACS and RNA-seq analysis, performed by the Isacoff lab. B) Dissections of tails at the 22 somite stage in the *1020*:*Gal4+* line. Tails were dissected away at the third somite. Figure modified from Drew Friedmann.

Genes encoding Connexin proteins that were found in the RNA-seq dataset from the Isacoff lab were identified as genes-of-interest, along with the remainder of zebrafish homologues of the human electrical synapse gene *Cx36*, the main neuronal

Connexin in humans (Miller et al., 2017). We hypothesized that the fourth homologues *gjd1b*/Cx34.7 – might also act as an essential genes for electrical synapse formation in the developing spinal cord and therefore included it as a gene-of-interest.

Generating mutations using CRISPR/Cas9

To determine whether the RNA-seq-identified electrical synapse genes are involved in forming the first synapses, we used Clustered Regularly Interspaced Short Palindromic Repeats (CRISPR) and Cas9 enzyme that causes double-stranded breaks in DNA at the specified site to generate mutations (Figure 16). We designed single guide RNAs (sgRNAs) using CRISPRscan to target an exon in each of *gjc2*/Cx43.4 and *gjd4*/Cx46.8 (Table 2). sgRNAs were designed and synthesized using a previously published protocol (Shah et al., 2016). Custom oligos with a 5' T7 promotor sequence (5′-aattaatacgactcactata-3′), the nucleotides of the designed target site, and the sgRNA overlap loop sequence (5′-gttttagagctagaaatagc-3′) were synthesized and combined with an sgRNA loop oligo, which the Cas9 enzyme recognizes and binds (5′-gatccgcaccgactcggtgccacttttcaagttgataacggactagccttattttaacttgctatttctagctctaaaac-3′). A polymerase chain reaction (PCR) using Phusion High-Fidelity DNA Polymerase (NEB) was performed across these two oligos to yield a 120 base pair DNA guide oligo. sgRNAs to inject into the embryos were transcribed using the T7 Megascript kit (ThermoFisher).

Synthesized sgRNAs were combined with Cas9 protein (IDT) at a final concentration of 1600 pg/nL of Cas9 and 200 pg/nL of sgRNAs. 1 nL of the Cas9/sgRNA solution was injected into *zf206ET* (control) embryos at the one cell stage of development.

Cx36 family genes were mutated according to a similar protocol and the resulting mutations were characterized previously (Miller et al., 2017).

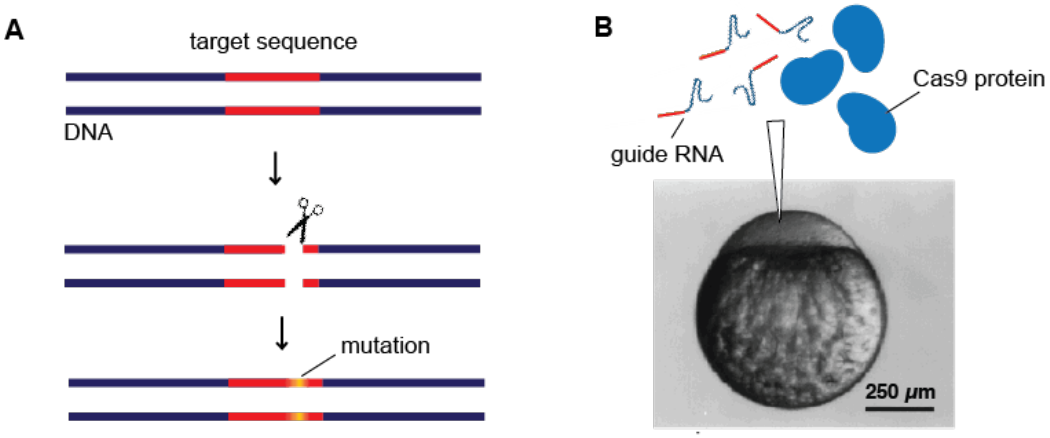

Figure 16. CRISPR/Cas9 mechanism for targeted mutations.

A) A target sequence within a gene is identified for mutation. Guide RNA complementary to the target sequence is designed and synthesized with a loop sequence for the Cas9 protein to identify. Once injected, Cas9, which acts like a pair of molecular scissors, creates a double-stranded break in the target sequence. The cells inherent genomic repair mechanisms attempt to repair the break, which usually results in several base pairs being lost. B) Guide RNA and Cas9 protein are injected into the embryo at the single cell stage. From Kimmel et al., 1995.

Table 2. sgRNA target sites for genes of interest.

gene	sgRNA sequence (target site)
gjd4/Cx46.8	5'- AATTAATACGACTCACTATAGGAGCGGAAGAGGGA CAGAGGTTTTAGAGCTAGAAATAGC-3'
gjc2/Cx43.4	5'- AATTAATACGACTCACTATAGGGCCATATCTTGCCC ACGAGTTTTAGAGCTAGAAATAGC-3'

Characterizing mutations using Sanger Sequencing and reverse transcription

Injected F0 embryos were raised until sexual maturity (three months) and outcrossed to wildtype *ABC* zebrafish. The offspring from these crosses were raised to 3

days post-fertilization (dpf) before their DNA was harvested after anesthesia using 4.2 mL of 4.0 g/L Tricaine (3-amino benzoic acidethylester) in 100 mL embryo medium. Full embryos were placed individually in 35 µL of base solution of 25 mM NaOH and 0.2 mM EDTA (pH 12) and lysed for 30 minutes at 95°C. DNA solutions were then brought to room temperature and neutralized using 40 mM Tris-HCl (pH 5).

PCR reactions using Taq DNA Polymerase amplified the genomic regions using primers (Table 3) around the predicted sites of mutagenesis. High resolution melt analyses (HRM) amplified the targeted regions and showed changes in how the gene's two DNA strands melt away from one another when heated. Deletions of base pairs cause the two strands to melt at lower temperatures. The melt data of the F1 DNA samples were compared with known wildtype genotypes to identify mutated genes at the target sites. The samples showing mutations were amplified around the genes-of-interest, purified using DNA Clean & Concentrator kits (Zymo Research), and sequenced using Genewiz Sanger Sequencing. Trace files were then analyzed using Geneious software v.9.1.3 to characterize the mutations.

Table 3. Genotyping primer sequences.

gene	type	forward	reverse
gjd4/Cx46.8	HRM	5'-GTTGTGCCAATGTGTGCTATGAC-3'	5'-CATTATGTAGGGGAGGCACAGAG-3'
	sequencing	5'-TCTACCAGGATGAGCAGGAACGA-3'	5'-TCGGTAGCTAAGCCAGAACTCACT-3'
gjc2/Cx43.4	HRM	5'-TTACGCGGTTGTTGGATGAAATC-3'	5'-CCCCACAACAGTCAAAACAATGC-3'
	sequencing	5'-AGAGGTGGTACTTCTTGAAGCA-3'	5'-CCGGACATGAGAGAGTGGTGCAA-3'
gjd1a/Cx34.1	HRM	5'-AGGTCGGCAGGGAAGTGAGAGT-3'	5'- ATAGAGCTCTTACCTGCCGATC-3'
	sequencing	5'-CACTAGAGTGCTGCCCTGACAC-3'	5'- ATAGAGCTCTTACCTGCCGATC-3'
gjd1b/Cx34.7	HRM	5'-CTTAAAGGATCGCTCGGTGTCT-3'	5'-TTCCGATCATAGTAGAGTGCTGCTG-3'
	sequencing	5'-GCCATCGGCGGAACTATTTTTA-3'	5'-TTCCGATCATAGTAGAGTGCTGCTG-3'
gjd2b/Cx35.1	PCR + restriction digest with BsaXI	5'-ATGATGATCTGGAAAACCCAGT-3'	5'-GGAGCAGATGTTCTTTGAGCTT-3'
	sequencing	5'-ATGATGATCTGGAAAACCCAGT-3'	5'-ATGATGATCTGGAAAACCCAGT-3'
gjd2a/Cx35.5	HRM	5'-GATGAGCAGCGATGGGAGAAT-3'	5'-CTTGAATTTCGGCGTCAGACAG-3'
	sequencing	5'-GAGAGGAGGGCTCACATGACTC-3'	5'-CTTGAATTTCGGCGTCAGACAG-3'

CRISPR/Cas9 injections generated multiple types of mutations of varying amounts of deleted or inserted base pairs. Mutations that were likely to be deleterious were selected based on probability of full gene knockout from **frame shifts,** resulting in complete changes to the translated amino acid makeup. To make sure that these deletions indeed resulted in protein knockout, we performed reverse transcription PCR (rt-PCR). This technique creates a **complementary DNA** (cDNA) library composed only of actively transcribed DNA using the preexisting RNAs as a template.

Seventy-five embryos of the *zf206ET* (control) and mutant lines were euthanized using Tricaine and pooled into 1.5 mL Eppendorf tubes. Embryo medium was removed and immediately replaced with 250 µL of Trizol (ThermoFisher Scientific). Cells were

lysed and homogenized using an RNase free pellet pestle until the tissue was sufficiently disrupted (approximately 30 strokes). An additional 750 µL of Trizol was added before incubating the samples for 5 minutes at room temperature to permit complete dissociation of nucleoprotein complexes. Following dissociation, 0.2 mL chloroform was added to all samples and tubes were rocked at room temperature for 15 seconds to mix. We then incubated the samples at room temperature for 2 minutes and centrifuged at 12,000 x g for 15 minutes at 4°C. This separated the mixture into a lower red phenol-chloroform phase, an interphase, and a colorless upper aqueous phase. The upper phase contained the extracted RNA and was subsequently transferred into a new 1.5 mL Eppendorf tube to be purified using a Zymo RNA Clean & Concentrator kit following the standard protocol with a slight modification. Following the RNA binding step, we prewashed the column with 400 µL RNA wash buffer. We centrifuged the column for 30 seconds above 11,000 x g and added DNase I reaction mix composed of 5 µL DNase I (Zymo Research) and 35 µL DNA digestion buffer. The columns were incubated at room temperature for 15 minutes before continuing with RNA purification as directed. Eluted RNA was stored at -80°C.

To synthesize the cDNA library, we combined 1 µL of 50 µg oligo(dt)20, 1 µL of 10 mM dNTP mix, and 5 µg total RNA to a 1.5 mL Eppendorf tube. Reaction mix was brought to 10 µL using DEPC-treated water. Tubes were then incubated at 65°C for 5 minutes and placed on ice for at least one minute. During incubation, cDNA synthesis mix was prepped separately in the following order: 2 µL of 10x RT buffer, 4 µL of 25 mM $MgCl_2$, 2 µL of 0.1 M DTT, 1 µL of 40 U/ µL RNaseOUT, and 1 µL of 200 U/ µL Superscript III RT (ThermoFisher). After incubation, each sample of RNA/Primer mix

was added to 10 µL of cDNA synthesis mix, gently mixed and collected via centrifugation, and incubated for 50 minutes at 50°C. Reactions were then terminated by incubating at 85°C for 5 minutes and then chilled on ice. Finally, we added 1 µL RNase H to each tube, incubated at 37°C for 5 minutes, and stored the cDNA at -20°C.

Using the resulting cDNA libraries as template DNA, PCR was performed with Taq DNA Polymerase using gene-specific primers. We then ran the resulting DNA products on a 2% electrophoresis agarose gel with SYBR Safe Stain (Invitrogen) to visualize nucleic acids.

Behavioral imaging and analysis

To analyze embryos for disrupted spontaneous coiling behavior, we embedded embryos in 1.4% low-melt agarose (Invitrogen) in embryo medium at 17 hpf. Embryos were oriented with their dorsal side flush with the petri dish, facing upwards. We then flooded the dish with embryo medium and removed the agar around the embryo's tail to allow freedom of motion while still maintaining a stationary position for imaging. A high-speed 5MP Monochrome CMOS Camera (Mightex Systems) was mounted below an elevated plastic sheet that held the embryo dish, allowing for imaging from below. A 6.5"x6.5" Ultra Thin LED Light Panel with Daylight White Light (Environmental Lights) was placed above the animals for back illumination (Figure 8). Mightex Systems software v1.2.1 was used to capture image sequences across time. Sequences of 2000 images of 2592 x 1944 pixel resolution with a 3 millisecond exposure time were captured at a frame rate of 6-7 frames per second. Each hour between 18 and 24 hpf we captured a sequence of 2000 images.

Sarah Stednitz (University of Oregon) developed software for behavioral preprocessing and collaborated with us to create imaging protocols. She coded a script in Python that screened through the entire sequence and subtracts out background to better visualize the moving tail of the coiling fish. She then manually selects the regions of interest containing each fish and defines the beginning of the tail (at the base of the yolk sac). The software detects of contour and motion of the tail, which after background subtraction is the darkest region of the image. Center of mass is then calculated based on the contour and defined start of the tail.

Stednitz's preprocessing outputted the coordinates of the tip of the tail at each frame in an image sequence for every time point for each fish. I then used MatLab to create a script that analyzed the trunk angle during each coiling event. I used a rotation matrix to rotate each tail coordinate and normalize the top of the tail to the origin. Each inflection into $-x$ values represented left coils, while each inflection into $+x$ values represented right coils. The maximum angle was calculated for the maximum y-value given for each coiling event. Statistics were performed using Prism 7.

Glossary

axon: a long, threadlike portion of a neuron that conducts impulses from the cell body to the synaptic terminal

axon terminal: the end point of an axon, where synapses form with a postsynaptic cell

chemoaffinity: interactions between specific molecular markers that prompts wiring of neurons

complementary DNA (cDNA): DNA synthesized from a single-stranded RNA (messenger RNA); constitutes some portion of the transcriptome

Connexin: a protein subunit that forms a gap junction channel; each gap junction hemichannel is composed of 6 Connexins

dendrite: short, branching extensions of a neuron that generally receive electrical impulses from other cells and transmit them to the cell body

deoxyribonucleic acid (DNA): a self-replicating material that carries genetic information in an organism's cells; formed with nucleotide base pairs that ultimately encode protein structures

frameshift mutation: a genetic mutation caused by insertions or deletions of a number of nucleotides in a DNA sequence that is not divisible by three

gap junction channels: aggregates of intercellular channels that allow for direct cell-to-cell transfer of ions and other small molecules; composed of 6 Connexin proteins on either side of the pre- and postsynaptic cell

neurotransmitter: molecules that are released at the end of a nerve fiber when an electrical impulse arrives; diffuses across the synapse and triggers the action potential to continue in the postsynaptic cell

olig2: *oligodendrocyte lineage transcription factor 2*, a transcription factor that is expressed only in the central nervous system

postsynaptic cell: the neuron that receives electrical impulses from the presynaptic cell, transmitted across the synaptic cleft

presynaptic cell: the neuron from which an electrical impulse is transmitted across the synaptic cleft which is then received by the postsynaptic cell

progenitor cell: a cell that differentiates into more specific cell types

ribonucleic acid (RNA): nucleic acid messenger transcribed from DNA that generally carries information for protein synthesis

synapse: a junction between two neurons consisting of a microscopic gap

voltage-gated ion channels: class of membrane-crossing proteins that form channels that ions can pass through when activated by changes in the voltage in the local area. The voltage temporary alters the structure of the channel, allowing ions to flow in and out.

References

Andersen, S. L. (2003). Trajectories of brain development: Point of vulnerability or window of opportunity? In *Neuroscience and Biobehavioral Reviews* (Vol. 27, pp. 3–18). https://doi.org/10.1016/S0149-7634(03)00005-8

Belluardo, N., Trovato-Salinaro, a, Mudo, G., Hurd, Y. L., & Condorelli, D. F. (1999). Structure, chromosomal localization, and brain expression of human Cx36 gene. *J Neurosci Res*, *57*(5), 740–752. https://doi.org/10.1002/(SICI)1097-4547(19990901)57:5<740::AID-JNR16>3.0.CO;2-Z [pii]

Chang, Q., & Balice-Gordon, R. J. (2000). Gap junctional communication among developing and injured motor neurons. *Brain Research Reviews*. https://doi.org/10.1016/S0165-0173(99)00085-5

Courchesne, E., Pierce, K., Schumann, C. M., Redcay, E., Buckwalter, J. A., Kennedy, D. P., & Morgan, J. T. (2007). Mapping early brain development in autism. *Neuron*, *56*(2), 399–413. https://doi.org/10.1016/j.neuron.2007.10.016

De Carlos, J. A., & Borrell, J. (2007). A historical reflection of the contributions of Cajal and Golgi to the foundations of neuroscience. *Brain Research Reviews*. https://doi.org/10.1016/j.brainresrev.2007.03.010

DiMartino, A., Fair, D. A., Kelly, C., Satterthwaite, T. D., Castellanos, F. X., Thomason, M. E., … Milham, M. P. (2014). Unraveling the miswired connectome: A developmental perspective. *Neuron*. https://doi.org/10.1016/j.neuron.2014.08.050

Friedmann, D., Hoagland, A., Berlin, S., & Isacoff, E. Y. (2015). A spinal opsin controls early neural activity and drives a behavioral light response. *Current Biology*, *25*(1), 69–74. https://doi.org/10.1016/j.cub.2014.10.055

Goulding, M. (2009). Circuits controlling vertebrate locomotion: moving in a new direction. *Nature Reviews. Neuroscience*, *10*(7), 507–518. https://doi.org/10.1038/nrn2608

Hatler, J. M., Essner, J. J., & Johnson, R. G. (2009). A gap junction connexin is required in the vertebrate left-right organizer. *Developmental Biology*, *336*(2), 183–191. https://doi.org/10.1016/j.ydbio.2009.09.035

Higashijima, S., Masino, M. A., Mandel, G., & Fetcho, J. R. (2003). Imaging Neuronal Activity During Zebrafish Behavior With a Genetically Encoded Calcium Indicator. *Journal of Neurophysiology*, *90*(6), 3986–3997. https://doi.org/10.1152/jn.00576.2003

Hoch, W. (1999). Formation of the neuromuscular junction. Agrin and its unusual receptors. *European Journal of Biochemistry*. https://doi.org/10.1046/j.1432-1327.1999.00765.x

Hodgkin, A. L., & Huxley, A. F. (1952). A Quantitative Description of Membrane Current and its Application to Conduction and Excitation in Nerves. *J. Physiol.*, *117*, 500–544. https://doi.org/10.1016/S0092-8240(05)80004-7

Hormuzdi, S. G., Filippov, M. A., Mitropoulou, G., Monyer, H., & Bruzzone, R. (2004). Electrical synapses: A dynamic signaling system that shapes the activity of neuronal networks. *Biochimica et Biophysica Acta - Biomembranes*. https://doi.org/10.1016/j.bbamem.2003.10.023

Insel, T. R. (2010). Rethinking schizophrenia. *Nature*. https://doi.org/10.1038/nature09552

Kandel, E. R., Schwartz, J. H., & Jessell, T. M. (2000). *Principles of Neural Science*. *Neurology* (Vol. 3). https://doi.org/10.1036/0838577016

Kimura, Y., Hisano, Y., Kawahara, A., & Higashijima, S. (2014). Efficient generation of knock-in transgenic zebrafish carrying reporter/driver genes by CRISPR/Cas9-mediated genome engineering. *Scientific Reports*, *4*, 6545. https://doi.org/10.1038/srep06545

Knogler, L. D., Ryan, J., Saint-Amant, L., & Drapeau, P. (2014). A Hybrid Electrical/Chemical Circuit in the Spinal Cord Generates a Transient Embryonic Motor Behavior. *Journal of Neuroscience*, *34*(29), 9644–9655. https://doi.org/10.1523/JNEUROSCI.1225-14.2014

Landesman, Y., Postma, F. R., Goodenough, D. a, & Paul, D. L. (2003). Multiple connexins contribute to intercellular communication in the Xenopus embryo. *Journal of Cell Science*, *116*(Pt 1), 29–38. https://doi.org/10.1242/jcs.00182

Lefebvre, J. L., Sanes, J. R., & Kay, J. N. (2015). Development of Dendritic Form and Function. *Annual Review of Cell and Developmental Biology*, *31*(1), 741–777. https://doi.org/10.1146/annurev-cellbio-100913-013020

Marder, E., & Bucher, D. (2001). Central pattern generators and the control of rhythmic movements. *Current Biology*. https://doi.org/10.1016/S0960-9822(01)00581-4

Martens, M. B., Celikel, T., & Tiesinga, P. H. E. (2015). A Developmental Switch for Hebbian Plasticity. *PLoS Computational Biology*, *11*(7). https://doi.org/10.1371/journal.pcbi.1004386

Miller, A. C., Whitebirch, A. C., Shah, A. N., Marsden, K. C., Granato, M., O'Brien, J., & Moens, C. B. (2017). A genetic basis for molecular asymmetry at vertebrate electrical synapses. *eLife*, *6*. https://doi.org/10.7554/eLife.25364

Muto, A., Ohkura, M., Kotani, T., Higashijima, S., Nakai, J., & Kawakami, K. (2011). Genetic visualization with an improved GCaMP calcium indicator reveals spatiotemporal activation of the spinal motor neurons in zebrafish. *Proceedings of the National Academy of Sciences of the United States of America*, *108*(13), 5425–5430. https://doi.org/10.1073/pnas.1000887108

Nadarajah, B., Jones, A. M., Evans, W. H., & Parnavelas, J. G. (1997). Differential expression of connexins during neocortical development and neuronal circuit formation. *Journal of Neuroscience*, *17*(9), 3096–3111. Retrieved from http://www.ncbi.nlm.nih.gov/entrez/query.fcgi?cmd=Retrieve&db=PubMed&dopt=Citation&list_uids=9096144

Peinado, A., Yuste, R., & Katz, L. C. (1993). Extensive dye coupling between rat neocortical neurons during the period of circuit formation. *Neuron*, *10*(1), 103–114. https://doi.org/10.1016/0896-6273(93)90246-N

Ramon y Cajal, S. (1906). The structure and connexions of neurons. *Nobel Lectures: Physiology or Medicine 1901-1921 (1976)*, 220–253.

Rash, J. E., Kamasawa, N., Vanderpool, K. G., Yasumura, T., O'Brien, J., Nannapaneni, S., Nagy, J. I. (2015). Heterotypic gap junctions at glutamatergic mixed synapses are abundant in goldfish brain. *Neuroscience*, *285*, 166–193. https://doi.org/10.1016/j.neuroscience.2014.10.057

Roerig, B., & Feller, M. B. (2000). Neurotransmitters and gap junctions in developing neural circuits. *Brain Research Reviews*. https://doi.org/10.1016/S0165-0173(99)00069-7

Saint-Amant, L., & Drapeau, P. (2001). Synchronization of an embryonic network of identified spinal interneurons solely by electrical coupling. *Neuron*, *31*(6), 1035–1046. https://doi.org/10.1016/S0896-6273(01)00416-0

Schwiening, C. J. (2012). A brief historical perspective: Hodgkin and Huxley. *Journal of Physiology*. https://doi.org/10.1113/jphysiol.2012.230458

Shah, A. N., Davey, C. F., Whitebirch, A. C., Miller, A. C., & Moens, C. B. (2015). Rapid reverse genetic screening using CRISPR in zebrafish. *Nature Methods*, *12*(6), 535–540. https://doi.org/10.1038/nmeth.3360

Shen, K., & Cowan, C. W. (2010). Guidance molecules in synapse formation and plasticity. *Cold Spring Harbor Perspectives in Biology*. https://doi.org/10.1101/cshperspect.a001842

Siegel, D. J. (1999). The Developing Mind. *The Developing Mind*, 67–120. https://doi.org/10.1017/S0954579407070149

Swinburne, I. A., Mosaliganti, K. R., Green, A. A., & Megason, S. G. (2015). Improved Long-Term Imaging of Embryos with Genetically Encoded α-Bungarotoxin. *PLOS ONE*, *10*(8), e0134005. https://doi.org/10.1371/journal.pone.0134005

Tabor, K. M., Bergeron, S. A., Horstick, E. J., Jordan, D. C., Aho, V., Porkka-Heiskanen, T., Burgess, H. A. (2014). Direct activation of the Mauthner cell by electric field pulses drives ultrarapid escape responses. *Journal of Neurophysiology*, *112*(4), 834–844. https://doi.org/10.1152/jn.00228.2014

Tsai, N. P., Wilkerson, J. R., Guo, W., Maksimova, M. A., Demartino, G. N., Cowan, C. W., & Huber, K. M. (2012). Multiple autism-linked genes mediate synapse elimination via proteasomal degradation of a synaptic scaffold PSD-95. *Cell*, *151*(7), 1581–1594. https://doi.org/10.1016/j.cell.2012.11.040

von Maltzahn, J., Wulf, V., & Willecke, K. (2006). Spatiotemporal expression of connexin 39 and -43 during myoblast differentiation in cultured cells and in the mouse embryo. *Cell Commun Adhes*, *13*(1–2), 55–60. https://doi.org/P69717K421V45262 [pii]\n10.1080/15419060600631508

Warp, E., Agarwal, G., Wyart, C., Friedmann, D., Oldfield, C. S., Conner, A., … Isacoff, E. Y. (2012). Emergence of patterned activity in the developing zebrafish spinal cord. *Current Biology*, *22*(2), 93–102. https://doi.org/10.1016/j.cub.2011.12.002

Westerfield, M. (2000). *The Zebrafish Book. A Guide for the Laboratory Use of Zebrafish (Danio rerio), 4th Edition*. *book*.

Wilkinson, D. G. (1993). Whole mount in situ hybridization of vertebrate embryos. In *In Situ Hybridization* (pp. 75–83).

Wu, H., Xiong, W. C., & Mei, L. (2010). To build a synapse: signaling pathways in neuromuscular junction assembly. *Development*, *137*(7), 1017–1033. https://doi.org/10.1242/dev.038711